Adsorption (2014) 20:233–250
DOI 10.1007/s10450-014-9606-z

Physical adsorption characterization of nanoporous materials: progress and challenges

Matthias Thommes · Katie A. Cychosz

Received: 13 November 2013 / Revised: 25 January 2014 / Accepted: 28 January 2014 / Published online: 19 February 2014

Abstract Within the last two decades major progress has been achieved in understanding the adsorption and phase behavior of fluids in ordered nanoporous materials and in the development of advanced approaches based on statistical mechanics such as molecular simulation and density functional theory (DFT) of inhomogeneous fluids. This progress, coupled with the availability of high resolution experimental procedures for the adsorption of various subcritical fluids, has led to advances in the structural characterization by physical adsorption. It was demonstrated that the application of DFT based methods on high resolution experimental adsorption isotherms provides a much more accurate and comprehensive pore size analysis compared to classical, macroscopic methods. This article discusses important aspects of major underlying mechanisms associated with adsorption, pore condensation and hysteresis behavior in nanoporous solids. We discuss selected examples of state-of-the-art pore size characterization and also reflect briefly on the existing challenges in physical adsorption characterization.

Keywords Physical adsorption · Argon 87 K adsorption · Pore condensation · Hysteresis · DFT pore size distribution · Hierarchically structured materials

M. Thommes (✉) · K. A. Cychosz
Quantachrome Instruments, 1900 Corporate Dr, Boynton Beach, FL 33426, USA
e-mail: matthias.thommes@quantachrome.com

1 Introduction

Major progress has been made in recent years concerning the synthesis of nanoporous materials with tailored pore size and structure, controlled surface functionality, and their applications (e.g. for reviews see: Barton et al. 1999; Roth and Vartuli 2005; Zhao and Wang 2007; Hoffmann et al. 2006; Kleitz 2008; Hartmann and Jung 2010; Kresge and Roth 2013). Advances have also been made in the development and structural characterization of micro- and mesoporous materials such as mesoporous zeolites and hierarchically organized pore structures with an appropriate balance of micropores, mesopores, and macropores, the latter being required to ensure the transport of fluids to and from the smaller pores at a satisfactory rate (e.g. Mintova and Cejka 2007; Serrano et al. 2009; Na et al. 2011; Möller and Bein 2011; Pérez-Ramírez et al. 2011; Zhang et al. 2012; Li et al. 2013; Valiullin and Kaerger 2011). Recently, the synthesis of a novel class of alumina/silica transition metal based materials has been reported, which have pores between 1 and 2 nm, i.e. these novel materials bridge between zeolites and M41S materials (Shpeizer et al. 2006, 2010). A major point of interest are metal–organic framework materials (MOFs) and related nanoporous materials which offer a wide range of potential applications such as gas storage, separation, catalysis, and drug delivery (Li et al. 1999; Ferey 2007; Hirscher et al. 2010; Moellmer et al. 2010).

The development of these novel nanomaterials has led to challenges in the field of physical adsorption characterization and a comprehensive textural characterization is crucial for the optimization of novel systems used in many important existing and potentially new applications. In fact surface area, pore size and porosity are critical properties in the fields of catalysis, separation, gas and energy storage,

batteries, and many others. Detailed insights into the pore architecture are particularly important because they control transport phenomena and diffusional rates and govern selectivity in catalyzed reactions. Various experimental methods can be applied for this task including gas (physical) adsorption, small angle X-ray and neutron scattering (SAXS and SANS), mercury porosimetry, electron microscopy (scanning and transmission), thermoporometry, and NMR-based methods. Each method has a limited length scale of applicability for pore size analysis. An extensive overview of the different methods for pore size characterization and their application range was given by the International Union of Pure and Applied Chemistry (IUPAC; Rouquerol et al. 1994). Among these, gas adsorption is a popular one because it allows assessing a wide range of pore sizes including the complete range of micro- and mesopores (up to ca. 50 nm). The applicability of gas adsorption and complimentary experimental techniques for macropore analysis (pores >50 nm) has been addressed in a recent IUPAC technical report (Rouquerol et al. 2012). In addition, gas adsorption techniques are convenient to use, are not destructive, and are not that cost intensive as compared to some of the above mentioned ones.

Physisorption (physical adsorption) is widely used for the surface and textural characterization of nanoporous materials (e.g. for textbooks and reviews see: Gregg and Sing 1982; Rouquerol et al. 2013; Lowell et al. 2004; Neimark et al. 2008; Thommes 2004, 2010; Kaneko et al. 2012). Physisorption is a general phenomenon and occurs whenever an adsorbable gas (the adsorptive) is brought into contact with the surface of a solid (the adsorbent). The forces involved are the van der Waals forces. Physisorption in porous materials is governed by the interplay between the strength of fluid–wall and fluid–fluid interactions as well as the effects of confined pore space on the state and thermodynamic stability of fluids in narrow pores.

Based on the IUPAC recommendations from 1985 (Sing et al. 1985), pores are divided into three groups according to their diameter: micropores of widths less than 2 nm, mesopores of widths between 2 and 50 nm and macropores of widths greater than 50 nm. Since 1985 major progress in state-of-the art physical adsorption characterization has been made (for reviews, please see for instance Neimark et al. 2008; Thommes 2004, 2010), which are to a large extent related to: (i) the development of nanoporous materials with uniform, tailor-made pore structure (e.g. mesoporous molecular sieves as mentioned before), (ii) the development of high resolution experimental protocols for adsorption of various subcritical fluids such as nitrogen at 77.4 K, argon at 87.3 K, and carbon dioxide at 273.1 K, and (iii) the development and application of microscopic approaches such as density functional theory (DFT) of inhomogeneous fluids, as well as methods based on molecular simulation (Gubbins 1997). These modern theoretical and computational methods, which are based on the statistical mechanics of nanophases, describe the configuration of adsorbed fluid (the adsorbate) on a molecular level (for a recent review see Monson 2012). It has been shown that the application of DFT methods allows one to obtain reliable pore size distributions over the complete range of micro- and mesopores (for a recent review on the application of DFT methods for pore size analysis see Landers et al. 2013). It should be noted that the pore size analysis depends explicitly on the choice of pore model. Methods for pore size analysis based on DFT and molecular simulation are now widely used and are commercially available for many important adsorptive/adsorbent systems and featured in an ISO standard (ISO 15901-1). It is evident that the above mentioned progress requires the update and extension of the before mentioned 1985 IUPAC recommendations and technical report dedicated to physical adsorption characterization. As a consequence, a new IUPAC task group is currently working on the necessary revisions of the 1985 report and it is expected that a new, updated technical report will be published in 2014 (for more information, please see http://www.iupac.org/web/ins/2010-009-1-100). This also includes amendments of certain key features of the 1985 report such as the classification of pore size, adsorption isotherms, and hysteresis loops.

Despite the mentioned progress made in physical adsorption characterization in recent years, major challenges still exist. Within this context major efforts have been made since ca. 2005 concerning the investigation and assessment of surface roughness on adsorption measurements and advances have been made here in particular with regard to improving the characterization of disordered nanoporous carbons (Thommes et al. 2012a, we discuss this in much detail in Sect. 4 of this paper). However, understanding the effects of roughness is a general problem for nanoporous materials (e.g. silica, porous silcon etc.) and this is still under investigation (e.g. Naumov et al. 2008; Grosman 2008; Myasaka et al. 2012; Tanaka et al. 2013). There are also still major challenges concerning the assessment of surface chemistry. Within this context, water adsorption is being investigated as a potential method (Kaneko et al. 1999; Lodewyckx and Vansant 1999; Stoeckli and Lavanchy 2000; Ohba et al. 2004; Liu and Monson 2005; Thommes et al. 2011, 2012b, 2013; Lodewyckx et al. 2013; Horikawa et al. 2011). In addition, more work is needed to investigate the pore network characteristics of nanoporous materials, in particular for materials with hierarchical pore structure. The development of more realistic adsorbent/pore models (beyond the widely applied single pore model) is here important (for reviews see Gelb

et al. 1999; Coasne et al. 2013). One also needs to stress the importance of coupling gas adsorption with other experimental techniques such as X-ray and neutron scattering based techniques, for studying details of the adsorption and phase behavior of fluids in complex pore networks (Sel et al. 2007; Mascotto et al. 2009; Jähnert et al. 2009; Findenegg et al. 2010; Myasaka et al. 2012).

Another challenge for physical adsorption characterization is to understand and take into account adsorption induced deformation effects on the adsorbent (Reichenauer and Scherer 2000; Shen and Monson 2002; Gor and Neimark 2011; Gor et al. 2013). Elastic deformation effects are relatively small and have been observed for various porous materials such as activated carbon, charcoal, porous glass, aerogel, porous silicon, and polymers of intrinsic microporosity (PIMs). Whereas elastic deformation does not significantly affect the adsorption isotherms with the exception of some polymers and high porosity materials (e.g. aerogels), major problems are associated with the characterization of soft materials where the adsorbent undergoes a phase or structural change during the adsorption process. In fact, the theories of adsorption and the corresponding methods for pore size analysis discussed in this article are based on the assumption that the adsorbent properties do not change in the process of adsorption, i.e. the shape of the adsorption isotherm is entirely associated with the adsorption and phase behavior of the adsorbate. Hence new challenges are associated with the characterization of flexible metal organic framework materials (MOFs) and related materials (for a review see Ferey 2007). The adsorption behavior of flexible MOFs requires the development of new theoretical approaches (Neimark et al. 2010). By applying the standard methods of pore size analysis, the steps in the adsorption isotherms caused by structural transformation of the adsorbent would be associated with pore filling giving rise to artificial peaks in the pore size distributions. These challenges need to be addressed in future work with advanced theoretical, computational, and experimental approaches applied on well-chosen model materials.

In this article we focus on selected, important aspects concerning the structural characterization of rigid, nanoporous materials by gas adsorption, but it should be noted that this work does not represent a comprehensive review of the field of physical adsorption characterization. This paper is also restricted to physical adsorption characterization based on subcritical fluids and does not address aspects of supercritical fluid adsorption. Indeed, some complimentary, but quite limited surface and pore structure information can be obtained from adsorption studies with supercritical fluids (e.g. Aranovich and Donohue 1997; Jagiello and Thommes 2004) but discussing this topic is beyond the scope of this brief review.

2 Experimental aspects

The most frequently used methods for physical adsorption analysis are the volumetric (manometric) and gravimetric methods. The gravimetric method is based on a sensitive microbalance and a pressure gauge. This method is convenient to use for the study of adsorption not too far from room temperature, but has deficiencies for adsorption measurements at cryogenic temperatures such as the boiling temperature of nitrogen and argon (77 and 87 K, respectively), which are primarily used for surface area and pore size characterization. The standard technique for such experiments is the manometric technique which is based on calibrated volumes and pressure measurements and uses the general gas equation of state. The adsorbed amount is calculated by determining the difference of the total amount of gas admitted to the sample cell with the adsorbent and the amount of gas in the dead space. Experimental details of the manometric method are described in various textbooks (e.g. Gregg and Sing, 1982; Rouquerol et al. 2013; Lowell et al. 2004), hence we do not discuss these details within the scope of this article.

Prior to the adsorption experiment, it is required to remove all physically adsorbed material from the adsorbent surface while avoiding irreversible changes to the surface. In principle, this can be accomplished by vacuum pumping or purging with an inert gas at elevated temperatures. Particularly for microporous materials, outgassing under vacuum is desirable as the adsorption measurements often start at relative pressures as low as 10^{-7}. This can again be achieved by using a turbomolecular pump which, if coupled with a diaphragm roughing pump, allows the sample to be outgassed even in a completely oil free system.

The proper choice of adsorptive is also crucial for an accurate and comprehensive pore structural analysis. For many years, nitrogen adsorption at 77 K has been generally accepted as the standard method for both micropore and mesopore size analysis, but for several reasons it is now becoming evident that nitrogen is not an entirely satisfactory adsorptive for assessing the micropore size distribution. It is well known that the quadrupole of the nitrogen molecule is largely responsible for the specific interaction with a variety of surface functional groups and exposed ions. This not only affects the orientation of the adsorbed nitrogen molecule on the adsorbent surface, but it also strongly affects the micropore filling pressure. For example, for many zeolites and MOFs, the initial stage of physisorption is shifted to extremely low pressures (to $\sim 10^{-7}$) where the rate of diffusion is extremely slow, making it difficult to measure equilibrated adsorption isotherms. Specific interactions with surface functional groups cause the problem that the pore filling pressure is not correlated with the pore size in a straightforward way. In

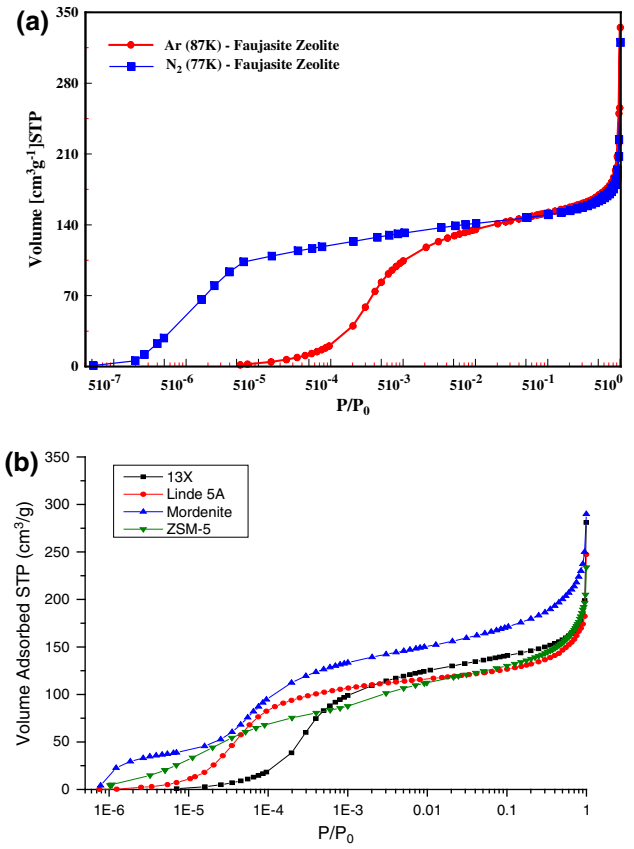

Fig. 1 **a** Nitrogen (77 K) and argon (87 K) adsorption isotherms on faujasite zeolite as a function of relative pressure, P/P_0, where P_0 reflects the saturation pressure. Adapted from Thommes (2007). **b** Argon adsorption (87 K) on various zeolites (semi-logarithmic scale)

contrast to nitrogen at 77 K, argon at 87 K (liquid argon temperature) does not exhibit specific interactions with surface functional groups. As a consequence of this and the slightly higher temperature, argon at 87 K fills micropores of dimensions 0.5–1 nm at significantly higher relative pressures compared to nitrogen at 77 K, leading to accelerated diffusion and faster equilibration time. The pore filling pressure of argon (87 K) is often shifted 1–1.5 decades in relative pressure as compared to nitrogen (Thommes 2007; Lässig et al. 2011; Silvestre-Albero et al. 2012). A comparison of argon (87 K) adsorption and nitrogen (77 K) adsorption for a faujasite zeolite is shown in Fig. 1a (Thommes 2007).

Argon adsorption at 87 K allows one to obtain high resolution adsorption isotherms in order to resolve small differences in texture; in fact, such argon (87 K) isotherms can be a considered a fingerprint of the pore structure. Examples of high resolution argon (87 K) adsorption isotherms are shown in Fig. 1b for various zeolites, i.e. H-mordenite, 13X, Linde 5A, and ZSM-5. In order to reveal the details of the low pressure region where micropore filling occurs, the isotherms are displayed in a semi-logarithmic scale of relative pressures. It can be clearly seen that the argon (87 K) isotherm into H-mordenite reveals two "steps" indicating pore filling of the main channels (0.67 nm × 0.7 nm) with 12-member ring windows (relative pressure range from 5×10^{-7} to 3×10^{-6}) and the 8-membered ring side pockets (relative pressure range from 1×10^{-5} to 1×10^{-3}). Figure 1b also clearly reveals that pore filling of the ZSM-5 pore channels (0.51 nm × 0.55 nm) occurs as to be expected between the two pore filling regions of H-mordenite. These data demonstrate clearly the potential of argon adsorption at 87 K to resolve small differences in pore size with a resolution of at least 0.1 nm (Thommes 2007). It should be noted that it is possible to achieve liquid argon temperature by using commercially available cryo-coolers or simple cryostats.

The question arises whether the advantages of argon adsorption at 87 K will be also present at liquid nitrogen temperature (77 K). Unfortunately, argon adsorption at 77 K is less than optimal for both pore size and surface area analysis because (i) a combined and complete micro- and mesopore size analysis with argon is not possible at 77 K (which is ca. 6.5 K below the triple point temperature of bulk argon) and is limited to pore diameters smaller than ca. 15 nm (for details see Thommes et al. 2002); (ii) although the argon adsorption isotherm at 77 K is still shifted to higher relative pressures as compared to nitrogen adsorption, the shift towards higher absolute pressure is less pronounced as compared to argon adsorption at 87 K and adsorption into narrow micropores still occurs below a relative pressure of 10^{-5} where the adsorption kinetics are very slow. This is due to the low saturation pressure of argon at 77 K (205 torr for solid argon and 230 torr for supercooled liquid argon, i.e. in many cases one can assume that argon confined to narrow pores is in a supercooled state). Hence, argon adsorption at 77 K does not offer the same experimental benefits as argon adsorption at 87 K.

Despite the advantages which argon adsorption at 87 K offers, there exists still the well-known problem of restricted diffusion, which prevents nitrogen and also argon molecules from entering the narrowest micropores—pores of width <0.45 nm. In carbon materials (where specific interactions are minimized), the use of CO_2 as adsorptive at temperatures close to room temperature has been suggested. At 273 K for instance, CO_2 is ca. 32 K below its critical temperature and because the saturation pressure is very high (26,200 torr), the relative pressure measurements necessary for the micropore analysis are achieved in the range of moderate absolute pressures (1–760 torr). Hence, due to the relatively high absolute temperatures and pressures compared with nitrogen and argon adsorption at cryogenic temperatures it has been established that

diffusion limitations of nitrogen in micropores can be eliminated by the use of CO_2 (Garrido et al. 1987; Cazorla-Amorós et al. 1996; García-Martínez et al. 2000). CO_2 molecules are able to easily access the ultramicropores despite the fact that the dimensions of N_2, Ar, and CO_2 are similar. Furthermore, the experimental setup needed to perform micropore analysis with CO_2 is much simpler than the corresponding experimental setup for micropore analysis by argon or nitrogen adsorption because a turbomolecular pump and low-pressure transducers are not necessary. Because of these experimental advantages, CO_2 adsorption has become a standard tool for the assessment of the ultramicroporosity of carbons for the pore width range <1 nm, which corresponds to a relative pressure (P/P_0) of 3×10^{-2} (i.e. ca. 1 bar of absolute pressure which is the highest pressure reachable in adsorption equipment typically used for characterization). Consequently, advanced DFT and Grand Canonical Monte Carlo (GCMC) methods have been developed for calculating the pore size distribution from the CO_2 adsorption isotherms (Ravikovitch et al. 2000; Vishnyakov et al. 1999).

One of the main advantages for performing CO_2 adsorption experiments at 273 K is that, because of the enhanced kinetics, a micropore characterization with CO_2 can be performed in a few hours; much faster than adsorption experiments at cryogenic temperatures. However, it should be noted that in particular for carbons with very narrow pores (e.g. carbon molecular sieves) the experimental equilibration parameters still have to be chosen carefully to assure the measurement of equilibrated adsorption data (Rios et al. 2007). The kinetics of CO_2 adsorption in carbon micropores has also been investigated by combining adsorption experiments with small angle X-ray scattering (Reichenauer 2005). Additionally, similar to nitrogen, CO_2 has a quadrupole moment, which affects the adsorption behavior on carbons containing oxygen surface functionalities as well as other oxidic materials such as zeolites, silicas, and MOFs, complicating the pore size analysis by CO_2 for such materials (Furmaniak et al. 2010). However, CO_2 adsorption can still be useful for assessing the pore volume/porosity for materials which have pores which cannot be assessed by nitrogen or argon. This has been demonstrated for a series type A zeolites (García-Martínez et al. 2000). The pore size in zeolite NaA is $\sim$0.4 nm and the results of the study confirm that N_2 molecules cannot enter the pores. However, useful CO_2 adsorption isotherms at 273 K could be obtained on NaA and the micropore volume calculated from the CO_2 adsorption data was found to be in good agreement with the values obtained from X-ray diffraction. Thus, CO_2 adsorption reliably provides a measurement of the volume of narrow micropores, but it needs to be stressed that its use for pore size analysis of adsorbents with polar surfaces, including carbons with oxidic functionality, is limited because of the specific interactions caused by the large quadrupole moment.

Krypton adsorption at 77 K has become a standard tool for low surface area analysis of materials (Lowell et al. 2004). By using highly accurate manometric (volumetric) adsorption equipment, it is possible to determine surface areas as low as $\sim$0.5–1 m^2 with nitrogen or argon as the adsorptive. In order to evaluate even lower surface areas, krypton adsorption at 77 K is generally applied. However, similar to argon 77 K, krypton is well below (by ca. 38 K) its triple point and sublimates at ca. 1.6 torr. For the BET analysis one usually assumes that the condensed adsorbate corresponds to a supercooled liquid ($P_0 = 2.63$ torr). Due to the extremely low saturation pressure, the number of molecules in the free space of the sample cell is significantly reduced (to 1/300th) as compared to nitrogen or argon at their respective boiling temperatures; this leads to the high sensitivity of krypton adsorption at 77 K. Krypton adsorption at 77 K is more or less exclusively used for low surface area analysis although some attempts to apply it or pore size analysis have been reported as well (Pauporté and Rathousky 2007). An empirical method based on krypton adsorption at 87 K has been developed and applied for pore size analysis of thin mesoporous oxidic films (Thommes et al. 2007, Krause et al. 2011). Although krypton at 87 K is 30 K below the bulk triple point temperature, if confined to oxidic pores there is indication that krypton at 87 K (contrary to at 77 K) still exists in a super-cooled liquid state up to a diameter <ca. 9 nm (Hung et al. 2007); aspects of the phase and sorption behavior of fluids below the bulk triple point temperature are also discussed in a very recent review article (Coasne et al. 2013).

3 Adsorption mechanism

In order to obtain surface area, pore size distribution, pore volume, and other structural information of materials with hierarchical pore structure from the analysis of gas adsorption isotherms it is necessary to understand the underlying, often quite complex, adsorption mechanisms. The mechanisms of micro- and mesopore filling differ substantially. The filling of micropores is, in most cases, a continuous process. A basic understanding of the micropore filling process has already been achieved by Dubinin and co-workers based on the pioneering work of Polanyi (see Gregg and Sing 1982; Rouquerol et al. 2013; Lowell et al. 2004).

The filling of narrow micropores (i.e. the 'ultramicropores' of width no more than two or three molecular diameters) occurs at low relative pressures ($P/P_0 < 0.01$) and is entirely governed by the enhanced fluid–solid

interactions. However, in addition to the strong adsorption potential, a cooperative mechanism including both fluid–solid interactions and fluid–fluid interactions plays a role in the pore filling process of wider micropores (i.e. supermicropores); this occurs in a range of higher relative pressure (e.g. $P/P_0 = 0.01$–0.15). The relative pressure at which micropore filling occurs depends on a number of factors including the size and nature of adsorptive molecules, pore shape, and effective pore width. The pore filling capacity depends on the accessibility of the pores for the probe molecules, which is determined by the molecular size and chosen experimental conditions.

Mesopores fill via pore condensation, which represents a first order gas–liquid phase transition. The sorption behavior in mesopores depends not only on the fluid–wall attraction, but also significantly on the attractive fluid–fluid interactions. This leads to the occurrence of multilayer adsorption and capillary condensation. Pore condensation represents a phenomenon whereby gas condenses to a liquid-like phase in pores at a pressure less than the saturation pressure, P_0, of the bulk fluid. It represents an example of a shifted bulk transition under the influence of the attractive fluid–wall interactions. Pore condensation is very often accompanied by hysteresis which is observed in single pores as well as in pore networks.

Traditionally, pore condensation has been described within the concept of the Kelvin approach (see Gregg and Sing 1982; Rouquerol et al. 2013; Lowell et al. 2004 and references therein). For pores of uniform shape and width (ideal slit-like or cylindrical mesopores), the shift of the gas–liquid phase transition of a confined fluid from bulk coexistence is expressed in macroscopic quantities like the surface tension of the bulk fluid, the densities of the coexistent liquid, and the contact angle of the liquid meniscus against the pore wall. However, these macroscopic concepts break down for more narrow mesopores. The Kelvin approach does not allow for the effect of the adsorption forces on pore condensation and does not correctly describe the underlying mechanism of pore condensation and hysteresis (i.e. the occurrence of delayed condensation due to metastable pore fluid as we will discuss in the next section). In contrast to the Kelvin approach, the Broekhoff and de Boer approach (1967a, b, 1968a, b) as well as the Saam–Cole theory (1974) capture the mechanism of pore condensation and hysteresis. However, all these classical methods fail to correctly describe the peculiarities of the pore critical region, confinement-induced shifts of the phase diagram of condensed fluid, and hysteresis behavior, specifically the disappearance of hysteresis with decreasing pore size (at a given temperature) or increasing temperature (for a given pore size) (for reviews where these phenomena are discussed, see Gelb et al. 1999; Thommes 2004; Monson 2008). In

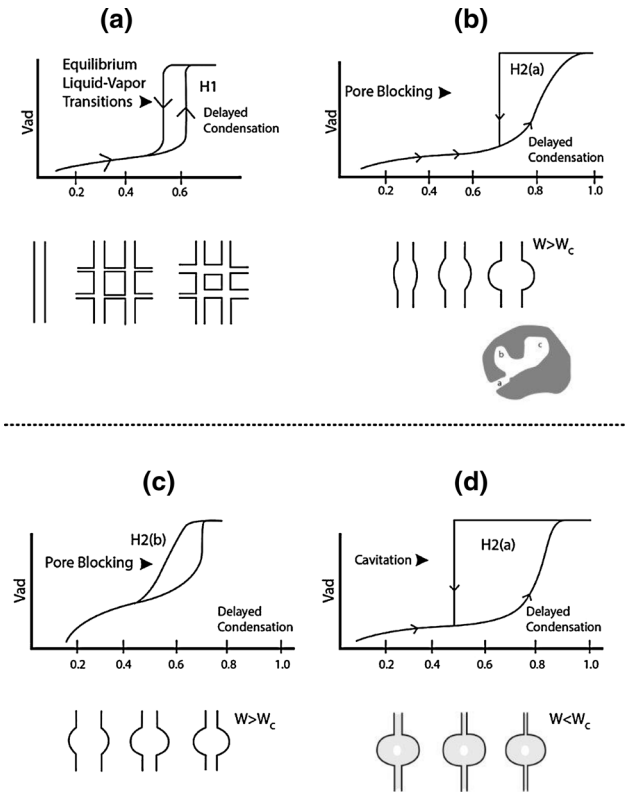

Fig. 2 Adsorption hysteresis types and their correlation with pore structure coupled with underlying adsorption mechanism. **a** Type H1 hysteresis, **b** type H2a hysteresis in materials with a wide distribution of pore body size, **c** type H2b hysteresis in materials with a wide distribution of pore neck size, and **d** type H2a hysteresis illustrating cavitation in a pore system with very narrow necks

contrast, it has been shown that modern, microscopic approaches such as DFT (NLDFT and QSDFT) and molecular simulation (GCMC) are capable of qualitatively and quantitatively predicting the pore condensation and hysteresis behavior of fluids in highly ordered model materials (for recent reviews see Monson 2012; Landers et al. 2013; Coasne et al. 2013). Progress has also been achieved in understanding the underlying internal dynamics of hysteresis in disordered pore systems (Valiullin et al. 2006), however, a discussion of this topic is beyond the scope of this paper.

It is widely accepted that there is a correlation between the shape of the hysteresis loop and the texture of the adsorbent. An empirical classification of hysteresis loops (into types H1, H2, H3, H4) was given by IUPAC in 1985 (Sing et al. 1985) and will be amended in the forthcoming IUPAC classification as mentioned in the introduction. Some characteristic hysteresis loops and their correlation with pore structure are given in Fig. 2. Hysteresis can be observed in single pores as well as in pore networks. A classical scenario of capillary condensation implies that the vapor–liquid transition is delayed due to the existence of

metastable adsorption films associated with nucleation barriers for the formation of liquid bridges. In an open pore filled by liquid-like condensate, the liquid–vapor interface is already present and evaporation/desorption occurs without nucleation, via a receding meniscus. That is, the desorption process is associated with the equilibrium vapor–liquid transition (e.g. Neimark and Ravikovitch 2001; Monson 2008). This mechanism leads to type H1 hysteresis which is dominant in ordered mesoporous materials with uniform cylindrical pores (e.g. MCM-41, SBA-15 silica), ordered three dimensional pore networks (such as MCM-48 and KIT-6 silica), and even some controlled pore glasses, (e.g. for adsorption hysteresis in controlled pore glass see Findenegg et al. 1994; Thommes and Findenegg 1994; Thommes et al. 2002; Thommes 2004).

In materials which exhibit more complex pore systems such as pore networks with ink-bottle shape pores, pore evaporation/desorption is also delayed and the wide body of the pore remains filled until the neck evaporates at a lower vapor pressure. This leads to type H2 hysteresis. For very disordered materials, the desorption branch of the hysteresis loop can be significantly steeper than the adsorption branch due to the fact that pore blocking induced evaporation represents a percolation transition (Fig. 2b). In this case the confined liquid evaporates from the pore system when the liquid from the largest neck evaporates. This results in a hysteresis loop of type H2a, which is also observed in the case where the size distribution of pore cavities is relatively wide compared to the distribution of neck sizes (Fig. 2b). In order to describe hysteresis phenomena in more disordered adsorbents, network models have been developed (e.g. Mason 1982; Wall and Brown 1981; Neimark 1991; Parlar and Yortsos 1988; Liu et al. 1993; Liu and Seaton 1994; Rojas et al. 2002). In the absence of percolation effects and in the case of a narrow size distribution of pore cavities, type H2b hysteresis is observed (Fig. 2c); type H2b hysteresis has, for instance, been observed for hydrothermally treated SBA-16 or KIT-5 silica. In this case, the analysis of the desorption branch allows one to obtain the pore size distribution of the pore entrances. Recent studies using model materials containing well-defined ink-bottle pores such as SBA-16, hierarchically ordered porous materials such as KLE, etc. (e.g. Woo et al. 2001; Sarkisov and Monson 2001; Ravikovitch and Neimark 2002a, b; Vishnyakov and Neimark 2003; Libby and Monson 2004; Thommes et al. 2006; Morishige et al. 2006; Nguyen et al. 2013a, b) revealed that if the pore neck diameter is smaller than a certain critical size at a given temperature and adsorptive, desorption occurs via cavitation, or, spontaneous nucleation of a bubble in the pore. In this case, the pore body empties, while the pore neck remains filled (Fig. 2d). For nitrogen and argon adsorption at 77 and 87 K, respectively, the critical neck width lies at 5–6 nm (Thommes et al. 2006; Ravikovitch and Neimark 2002a, b).

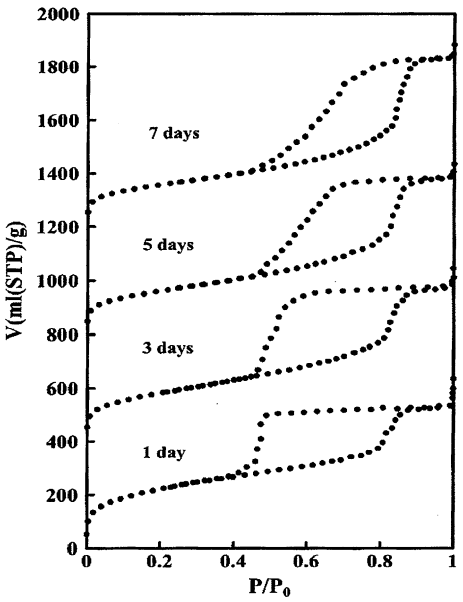

Fig. 3 Change from cavitation induced evaporation to pore blocking for N_2 (77 K) desorption in hydrothermally treated KIT-5 silica. From Morishige et al. (2006)

Hence, for a given temperature and adsorptive, the neck size dictates the desorption mechanism. Correspondingly, by varying the neck size or entrances to the main pore system, one should be able to observe such a transition from cavitation induced evaporation to pore blocking. Such results have been reported for instance for SBA-16 silica (Kim et al. 2004), FDU-1 silica (Kruk et al. 2005), and KIT-5 silica (Morishige et al. 2006). In the case of KIT-5 silica (KIT-5 silica is a highly ordered large-cage mesoporous silica with *Fm3m* close packed structure), the sample was hydrothermally treated for prolonged times, which resulted in an increase in the neck diameter. As shown in Fig. 3, with increasing neck diameter, a transition from cavitation to pore blocking controlled evaporation (note the appearance of "inverse type H2 hysteresis" as discussed in Fig. 2) is observed, which occurs after a hydrothermal treatment of KIT-5 silica for 5 days.

Not only does the pore neck width affect the transition from pore blocking to cavitation, but both temperature and the pore/cavity size (Rasmussen et al. 2010) can also have an effect on cavitation. It has been shown that the cavitation transition shifts to lower relative pressures with decreasing temperature (Ravikovitch and Neimark 2002b; Morishige et al. 2006; Thommes et al. 2006). Figure 4 demonstrates the pore cavity size dependence on the cavitation pressure. This figure contains data for silica materials with spheroidal mesopores (SBA-16, KLE, and SLN-326 type silica), but also two examples of silicas with cylindrical pores (SE3030).

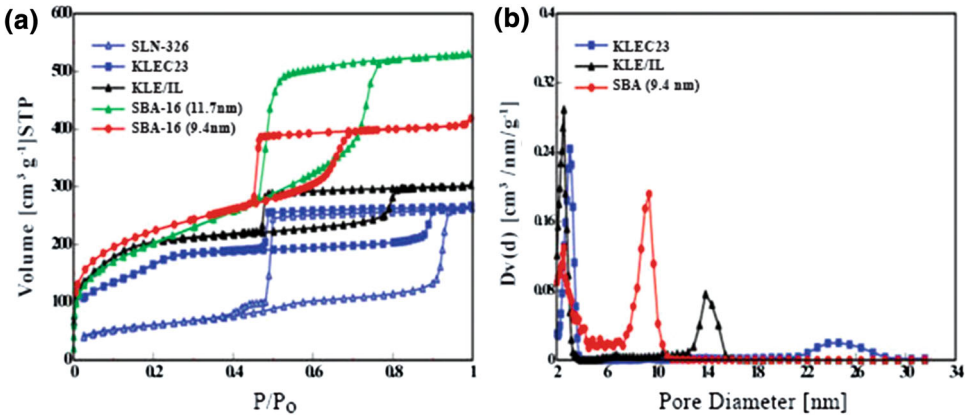

Fig. 4 **a** Nitrogen (77.4 K) adsorption in SBA-16 and hierarchically structured silica samples with main pore cavity diameters of >9.4 nm. **b** Selected NLDFT pore size distribution curves. From Rasmussen et al. (2010)

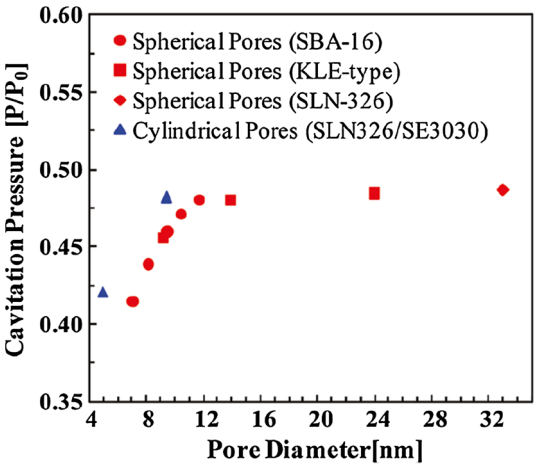

Fig. 5 Effect of pore diameter on cavitation pressure. Experimental data for samples with spheroidal pores are in red and cylindrical pores in blue. From Rasmussen et al. (2010)

In samples with pore sizes smaller than 11 nm, a noticeable shift is observed in the relative pressure range from 0.42 to 0.49 with increasing pore diameter. The cavitation in spheroidal pores increases almost linearly with the increase in pore diameter up to ~11 nm and then saturates in the range of pore diameters from 11 to 35 nm, i.e. no pore size effect on cavitation can be observed for pore sizes larger than ~11 nm (Fig. 5). These experimental observations were confirmed qualitatively by Monte Carlo simulations. These results are in line with the fact that as the confinement size decreases, the liquid spinodal, which determines the limit of metastability and the conditions of cavitation, shifts to lower pressure. On the other hand, it was hypothesized that the observed saturation of the pore size dependency on the cavitation pressure observed in pores of 11–35 nm indicates that in spherical cavities larger than 11 nm the conditions for bubble nucleation approach the nucleation conditions in the bulk liquid. Correspondingly, one could efficiently study cavitation stability in metastable bulk liquid by measuring desorption isotherms in materials with large mesopores.

In order to fully characterize a material, one needs to differentiate between equilibrium desorption, pore blocking, and cavitation mechanisms for the desorption data, i.e. in the case of pore blocking/percolation, information about the pore neck sizes can be obtained from the desorption branches which is not available in the case of cavitation. On the other hand, the occurrence of cavitation induced evaporation suggests that meso- and micropores are connected and that the larger mesopores are only accessible to narrower necks of pore diameter <5–6 nm. For a given pore system of fixed neck and pore cavity size, one expects to see a transition from pore blocking to cavitation by increasing the experimental adsorption temperature. This has been predicted by NLDFT (Ravikovitch and Neimark 2002b) and has also been demonstrated for hydrothermally treated KIT-5 silica (Morishige et al. 2006). This suggests the possibility of estimating the neck size distribution from the desorption isotherm by tuning the experimental conditions, such as temperature. Another possibility is to use various probe molecules and it has been demonstrated that adsorption experiments performed with different adsorptives (e.g. nitrogen and argon at 77 and 87 K, respectively) allow for detecting and separating the effects of pore blocking and cavitation over the course of evaporation (Thommes et al. 2006). This can help to determine neck sizes of materials, which is crucial for a comprehensive pore structure characterization, and is particularly important in many applications, because the pore necks control the accessibility of molecules into the porosity.

Complementary information about the underlying adsorption mechanism (desorption, cavitation, and pore blocking) and corresponding pore network characteristics such as pore connectivity, pore shape, etc. can be obtained by so-called hysteresis scanning (van Bemmelen 1897; DeBoer 1958; Everett 1967). After the measurement of the initial adsorption and desorption curves (boundary curves), one measures in subsequent cycles the adsorption/desorption isotherm only in the relative pressure range where hysteresis occurs (i.e. one does not completely fill the pore

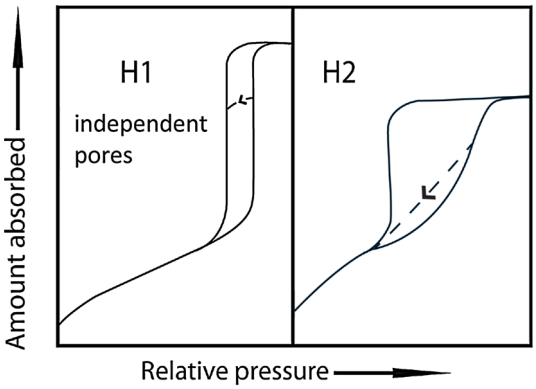

Fig. 6 Schematic illustration of desorption scanning in isotherms with Type H1 and Type H2 hysteresis

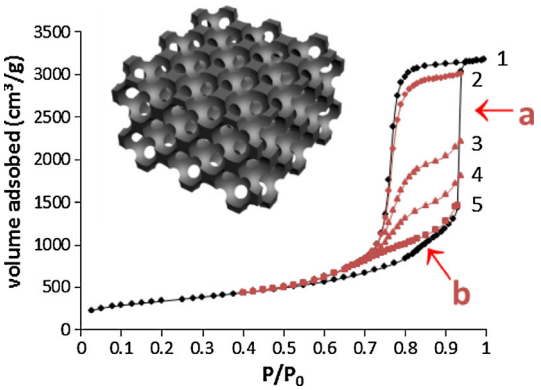

Fig. 7 Schematic representation and desorption scanning curves for the 40 nm 3DOm carbon. Adapted from Cychosz et al. (2012)

network system with condensate) and generates in this way desorption and adsorption scanning curves. Figure 6 illustrates the desorption scanning behavior typically observed for isotherms obtained on materials which consist of independent pores (with a finite pore size distribution), which exhibit type H1 hysteresis, or in disordered pore networks where the desorption branch is controlled by percolation effects leading to type H2 hysteresis. In the case of independent pores, only partially filling the pore system has no effect on the shape of the desorption scan. In contrast, in a material with type H2 hysteresis (a material where pore blocking is present), evaporation of certain pores depends on the state of neighboring pores leading to a desorption scan with a different shape than the initial desorption curve.

For instance, hysteresis scanning coupled with advanced network modeling was recently utilized for the characterization of three-dimensional ordered mesoporous (3DOm) carbons (Cychosz et al. 2012; Cimino et al. 2013). A 3DOm carbon templated to have 40 nm mesopores was analyzed using argon (87 K) hysteresis scanning (Fig. 7). Hysteresis scans reveal a pore structure comprised of two independent pore networks (labeled a and b in the figure). These two pore systems empty independently from each other and are not connected.

4 Surface area, pore volume, and pore size analysis

The standard method applied in physical adsorption characterization for surface area assessment is the BET (Brunauer, Emmett, and Teller) method and it continues to be the most widely used procedure for evaluating the surface area of porous and finely-divided materials, in spite of the weakness of its well- known shortcomings (Gregg and Sing 1982; Rouquerol et al., 2013, Lowell et al. 2004). Indeed, under certain, carefully controlled conditions, the BET area of a non-porous, macroporous, or mesoporous solid (i.e. materials which give rise to a type II or a type IV isotherm of the IUPAC classification, Sing et al. 1985) can be regarded as the probe accessible area or the effective area available for the adsorption of specified adsorptives. The application of the BET method on materials with micropores is not straightforward because it is impossible to separate the processes of monolayer–multilayer adsorption and micropore filling. With microporous adsorbents, the linear range of the BET plot, i.e. the range of relative pressures where the BET method should be applied, is often narrow and may be difficult to locate. A useful procedure was recently introduced (Rouquerol et al. 2007), which allows one to overcome this difficulty and determine the linear BET range in an unambiguous way. However, it should be stressed that the BET area derived from an isotherm obtained on microporous materials should not be treated as a realistic probe accessible surface area but rather as an apparent surface area.

Contrary to surface area assessment, the determination of pore volume and pore size is more straight-forward, even for microporous materials. Purely microporous materials exhibit a type I isotherm (according to the IUPAC classification) with a horizontal plateau. Also, mesoporous materials containing no macropores exhibit type IV isotherms, which remain nearly horizontal over the upper relative pressure range. For such cases, the pore volume, V_p, is then derived from the amount of vapor adsorbed at a relative pressure close to unity such as $P/P_0 = 0.95$, by assuming that the pores are filled with the adsorbate in the bulk liquid state and applying the Gurvich rule. If macropores are present, the isotherm is no longer nearly horizontal near $P/P_0 = 1$ and the total pore volume can no longer be evaluated (Gregg and Sing 1982; Rouquerol et al. 2013; Lowell et al. 2004).

Very often, microporous materials contain additional mesoporosity and in this case the micropore volume can be

obtained by applying the standard and comparison isotherm concepts (t-method, alpha-s method). These empirical methods allow one to determine micropore volume, external surface area, and, in principle, information about the average pore size. For carbon materials, methods based on the Dubinin–Radushkevich (DR) approach (Dubinin and Timofeev 1948; Dubinin and Radushkevitch 1947; Gregg and Sing 1982, Rouquerol et al. 2013) are frequently applied to obtain micropore volume. A more advanced method which allows for the determination of the micropore size distribution of microporous carbons up to a pore width of 2 nm was put forward by Horvath and Kawazoe (HK) and is based on work of Everett and Powl (Everett and Powl 1976; Horvath and Kawazoe 1983). The HK method allows for the calculation of the micropore volume distribution from a low pressure nitrogen adsorption isotherm obtained on a slit pore carbon. Later this approach was extended to argon (87 K) adsorption in zeolitic pores with cylindrical pore geometry (Saito and Foley 1991). An extension of the HK method for the characterization of zeolite spherical pores has also been developed (Cheng and Yang 1994). Contrary to the classical, Dubinin related approaches, the HK approach employs a realistic adsorption potential and provides a detailed account of the enhancement of the adsorption potential as the pore size decreases. The advantage of the HK and SF methods compared to methods based on Dubinin approaches is that they are specific with respect to the pore shape and adsorbate–adsorbent interaction potential. However, a disadvantage is that they do not give a realistic description of the micropore filling because they neglect the inhomogeneity of the adsorbed molecules in the micropores. In addition, similar to the Gurvich rule, DR, and comparison plot methods, the HK derived methods assume that the adsorbate phase is bulk-liquid like, i.e. these methods do not account for the fact that the degree of molecular packing in small pores depends on both the pore size and shape. These shortcomings can lead to significant inaccuracies in the pore size and volume determination.

Also, the modified Kelvin equation, which serves as the basis for many classical methods of mesopore analysis, including the widely used BJH (Barett, Joyner, Halenda) method (Gregg and Sing 1982), is based on macroscopic, thermodynamic assumptions. The Kelvin equation provides a relationship between the pore diameter and the pore condensation pressure and predicts that pore condensation shifts to a higher relative pressure with increasing pore diameter and temperature. As discussed in Sect. 3, the validity of the Kelvin equation becomes questionable for narrow mesopores because macroscopic concepts can no longer be applied. This had been clearly demonstrated by using model mesoporous molecular sieves (e.g. M41S materials) which allowed for the first time direct experimental tests of the validity of Kelvin equation based methods. Because of the high degree of order, the pore diameter of such model substances can be derived by independent methods (X-ray-diffraction, high-resolution transmission electron microscopy, etc.). It was found that the BJH method and related Kelvin equation based procedures may underestimate the pore size by up to 20–30 % for narrow mesopores smaller than ca. 10 nm if not properly corrected (for reviews see Neimark et al. 2003; Thommes 2004, 2010; Landers et al. 2013). Some improvement was achieved by calibrating the Kelvin equation using a series of mesoporous molecular sieves (MCM silicas) of known pore diameter over a limited pore diameter range of 2–10 nm (Kruk et al. 1997; Jaroniec and Solovyov 2006). However, these calibrated methods are only valid over a limited pore size range.

The problems associated with the above mentioned macroscopic, thermodynamic methods have been addressed by applying microscopic methods based on molecular simulation or DFT, which yield the thermodynamic and density profiles of confined fluids (for a recent review see Monson 2012) and describe details of the adsorbed phase on a molecular level. They capture the essential features of the pore filling mechanism of micropores and the mechanism of pore condensation, evaporation, and hysteresis. As a consequence they allow one to obtain (compared to the classical methods) much more reliable pore size distributions over the complete range of micro- and mesopores. Pioneering studies on DFT and the adsorption and phase behavior of fluids in pores were performed by Evans and Tarazona (Tarazona 1985; Tarazona and Evans 1984). Seaton et al. (1989) were the first to apply DFT for the calculation of the pore size distribution in both the micro- and mesopore ranges. In this first attempt, the pore size distribution analysis based on the local version of DFT was used. Although the local DFT provides a qualitatively reasonable description of adsorption in pores, it is quantitatively inaccurate especially in the range of micropores. A significant improvement in accuracy was obtained with the non-local density functional theory (NLDFT), which was first reported for the pore size analysis of microporous carbons in 1993 (Lastoskie et al. 1993) and was then further refined (Olivier et al. 1994; Neimark 1995). With these advanced methods it is now possible to obtain reliable information from both the adsorption and desorption branches of the hysteresis loop which is crucial for pore size characterization of materials consisting of an interconnected micro–mesoporous network. In fact, DFT based methods allow one to obtain the mesopore size from the adsorption branch by taking into account the delay in condensation due to metastable pore fluid (i.e. so called metastable adsorption branch DFT kernel; Ravikovitch and Neimark 2002a, b). It could be demonstrated that in the

absence of pore blocking effects or cavitation, (i.e. for some mesoporous molecular sieves where type H1 hysteresis is observed) the mean pore diameters obtained from both the adsorption branch (by applying the so-called metastable adsorption branch DFT method) and the desorption branch (by applying the equilibrium DFT method) were in good agreement (e.g. Ravikovitch and Neimark 2002a, b; Thommes 2004; Kleitz et al. 2010). On the other hand, for materials which give rise to pore blocking or cavitation a correct pore/cavity size distribution can be obtained by applying a proper DFT kernel (which correctly takes into account the delay in condensation) on the adsorption branch of the isotherm. Methods for pore size analysis based on DFT and molecular simulation are now widely used and are commercially available for many important adsorptive/adsorbent systems (for a recent review on the details of the DFT method and its application for pore size analysis, see Landers et al. 2013).

A drawback of the NLDFT method for the pore size characterization of disordered carbon materials is that the solid surface is treated as molecularly smooth and its predictions imply pronounced layering steps on adsorption isotherms, which are not observed in experimental adsorption isotherms on amorphous carbons. This can cause prominent artifacts in the NLDFT pore size distributions, such as the gap at ca. 1 nm, which is characteristic of many porous activated carbons (Ravikovitch et al. 2000; Olivier 1998). Several approaches have been suggested to account for the heterogeneity of carbon materials including the development of advanced structural models of porous carbons by reverse Monte Carlo techniques (e.g. Bandosz et al. 2003; Thomson and Gubbins 2000; Nguyen et al. 2008) which, however, are still too complex to be implemented for routine pore size analyses. Others suggested modeling porous carbons with a mixed geometry model (Soares Maia et al. 2011). Molecular simulations have also demonstrated that the surface roughness and defects significantly affect the shape of adsorption isotherms on heterogeneous surfaces (Do and Do 2006; Bakaev 1995; Turner and Quirke 1998; Lucena et al. 2010). Within the framework of the standard slit-pore model of carbons, variability of pore wall thickness was introduced (Bhatia 2002), but it led to just a marginal improvement over the standard NLDFT approach. The drawbacks of the conventional NLDFT model were also addressed by the introduction of two-dimensional DFT approaches which allow one to take into account effects of energetic heterogeneity as well as geometrical corrugation (Jagiello and Olivier 2009; Jagiello and Olivier 2013).

In order to account quantitatively for the effects of surface heterogeneity in carbons in a practical way, quenched solid density functional theory (QSDFT) was introduced. In contrast to the conventional NLDFT models that assume structureless graphitic pore walls, the solid is modeled using the distribution of solid atoms rather than the source of the external potential field. The surface heterogeneity in the QSDFT model is characterized by a single roughness parameter that represents the characteristic width of molecular level surface corrugations. The QSDFT method for carbons (Neimark et al. 2009) has originally been developed assuming slit-shaped pores, which are typical model pores in activated microporous carbons. However, due to the emergence of novel materials with pre-designed pore morphology obtained by synthesis routes which make use of structure directing agents or hard templates, the QSDFT method has recently been extended to micro–mesoporous carbons with cage-like and channel-like pore geometries (Gor et al. 2012). It has been shown that the QSDFT model significantly improves the reliability of the pore size analysis of microporous carbons (Neimark et al. 2009; Thommes et al. 2012a, Silvestre-Albero et al. 2012). This is also demonstrated in Fig. 8, which shows the application of both NLDFT and QSDFT on a nitrogen adsorption isotherm obtained on CMK-8 carbon (Thommes et al. 2013). CMK-8 carbon is an inverse replica of KIT-6 silica molecular sieve (Kleitz et al. 2003; Kleitz 2008). Figure 8a shows the theoretical fit of both the NLDFT and QSDFT methods based on a slit-pore carbon model to the experimental N_2 (77 K) data in a semilogarithmic scale. The QSDFT method, which takes into account the heterogeneity and surface roughness of the carbon, allows one to obtain a more reliable pore size distribution for these CMKs as compared to NLDFT which is also demonstrated in the almost perfect fit of the theoretical QSDFT isotherm to the experimental data as displayed in Fig. 8a. In contrast to QSDFT, the NLDFT isotherm reveals layering transitions in the relative pressure ranges from 10^{-5} to 10^{-3} and a less pronounced transition at a relative pressure of 0.1, which are expected for adsorption on perfectly smooth and chemically homogeneous surfaces. As a consequence one observes two artificial minima in the NLDFT pore size distribution (at ca. 1 and 2 nm), which are not observed in the QSDFT pore size distribution. The QSDFT pore size calculation indicates a narrow distribution of mesopores centered around 3 nm, as well as some microporosity which are also both observed with NLDFT; hence with the exception of the mentioned two artificial minima, the pore size distributions from NLDFT and QSDFT are in good agreement.

As mentioned before, the last decade has seen a lot of activity with regard to the development of materials with hierarchical pore structure as mentioned in Sect. 1 (e.g. Mintova and Cejka 2007; Serrano et al. 2009; Na et al. 2011; Möller and Bein 2011; Pérez-Ramírez et al. 2011; Zhang et al. 2012; Inayat et al. 2012; Li et al. 2013). The network of interconnected micro- and mesopores facilitates

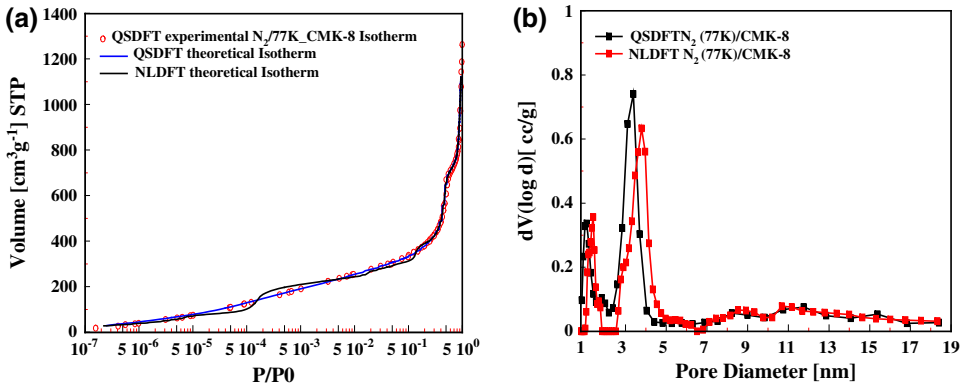

Fig. 8 **a** Nitrogen adsorption in CMK-8 carbon (semi-logarithmic plot) and **b** NLDFT vs. QSDFT pore size analysis. From Thommes et al. (2013)

efficient transfer of fluids to and from active sites located predominantly within the micropores. This has the potential to benefit a variety of processes in different areas including catalysis (Li et al. 2013), battery applications (Zhang et al. 2012), among others. An accurate textural characterization is crucial for optimizing these applications and hence we discuss below three selected, characteristic examples concerning the physical adsorption characterization of materials with hierarchical pore structure.

As discussed in Sect. 3, pore condensation and hysteresis observed in hierarchical micro–mesoporous structures are affected by various mechanisms. In addition to the delayed condensation due to metastable pore fluid, evaporation (desorption) of the liquid condensed in the pore bodies is in some cases delayed due to either pore blocking or cavitation (leading often to type H2 hysteresis). In this case, a valid pore size distribution curve can only be obtained from the adsorption branch by applying advanced NLDFT methods which (contrary to the Kelvin equation and other classical methods) take into account that the pore geometries of the micro- and mesopores might be quite different and that capillary condensation occurs delayed in the region of hysteresis. This is demonstrated in Fig. 9a, which shows nitrogen adsorption into KLE silica. KLE silica contains large spherical cavities of ca. 14 nm, which are connected through 1.3 nm wide micropores. Capillary evaporation/desorption occurs via cavitation (see Thommes et al. 2006) which leads to a wide hysteresis loop of type H2. Hence, no reliable, quantitative pore and neck size information can be obtained from the hysteretic region of the desorption branch, however the occurrence of cavitation induced evaporation indicates that there exists indeed ink-bottle type pores with neck diameters <5–6 nm. In such a case the pore size distribution has to be calculated from the adsorption branch with a method which takes into account the correct pore geometries and the existence of metastable pore fluid associated with the pore condensation process. Hence, the micro–mesopore size distribution shown in Fig. 9b was obtained by applying a hybrid NLDFT kernel on the adsorption branch of the isotherm, which correctly takes into account the delay in condensation (metastable adsorption branch NLDFT kernel). The applied NLDFT method is based on a cylindrical pore model for the micropore and narrow mesopore range and a spherical pore model for the mesopore range in which hysteresis is observed. The pore size data obtained in this way were in very good agreement with results obtained by advanced SAXS and TEM analyses (Thommes et al. 2006).

An example for the pore size characterization of MFI based zeolite with hierarchical pore structure is shown in Fig. 10 (Zhang et al. 2012). Figure 10a shows the high resolution TEM image of this ordered, potentially more efficient catalyst for the production of chemicals used in the plastics, biofuels, and pharmaceutical industries. Argon (87 K) adsorption isotherms were measured on this hierarchical zeolite structure for pure silica and aluminosilicates and one characteristic example is shown in Fig. 10b, along with the NLDFT fit to the experimental data that indicates the model is capable of accurately describing the adsorption behavior. A hybrid NLDFT method was applied which assumes argon adsorption in cylindrical siliceous zeolite pores in the micropore range and an amorphous (cylindrical) silica pore model for the mesopore range. The unique house-of-cards arrangement of these zeolite nanosheets provides a hierarchical pore network consisting of narrow micropores centered around 0.52 nm, typical of MFI zeolites and a broad distribution of mesopores (2–7 nm) for both the silica and aluminosilicate materials in good agreement with the TEM and XRD data shown in Fig. 10a. Cumulative NLDFT pore volume plots (Fig. 10c) confirm the hierarchical structure and allow one to differentiate between micro- and mesopore volume. This example demonstrates the usefulness of argon (87 K) adsorption coupled with advanced NLDFT for a reliable pore size analysis of the complete micro- and mesopore range.

Materials with hierarchical pore structure have also been shown to be superior for battery applications, including a microwave exfoliated graphene oxide that was characterized using a combination of nitrogen (77 K), argon (87 K),

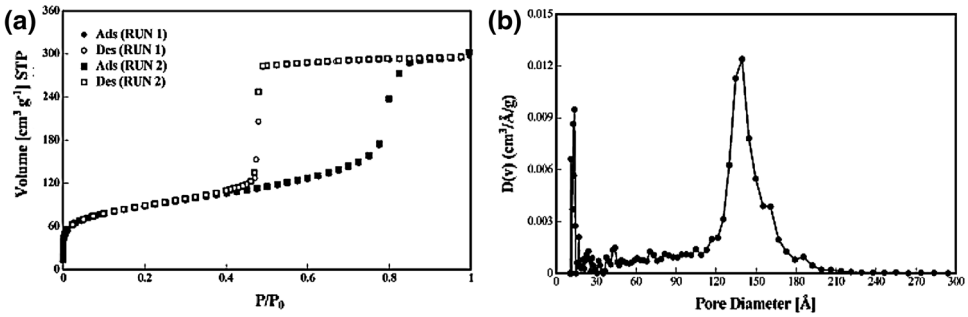

Fig. 9 **a** Nitrogen (77 K) adsorption isotherms for hierarchically structured micro-mesoporous KLE silica and **b** NLDFT pore size distribution calculated from the adsorption branch of the nitrogen (77 K) isotherm. Adapted from Thommes et al. (2006)

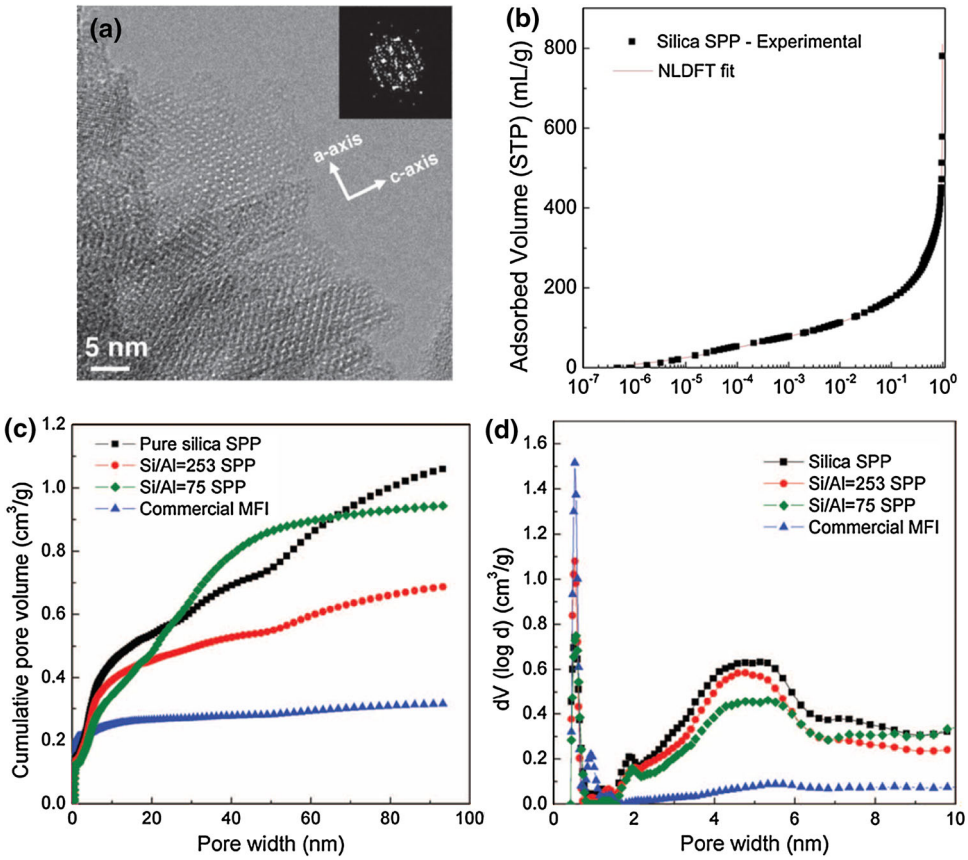

Fig. 10 **a** High resolution TEM image of a self-pillared zeolite nanosheet, **b** argon (87 K) adsorption isotherm of silica SPP zeolite with NLDFT fit, **c** argon NLDFT cumulative pore volumes over the entire pore size range, and **d** argon NLDFT pore size distributions up to 10 nm showing the narrow micropores and mesopores. From Zhang et al. (2012)

and carbon dioxide (273 K) adsorption (Zhu et al. 2011). This nice example, which demonstrates the complementary use of various adsorptives along with the proper use of DFT for calculation of pore size distribution in a graphene material, is shown in Fig. 11a. In the case of this carbon, the NLDFT pore size distribution calculated from the carbon dioxide adsorption isotherm clearly shows the presence of pores smaller than 0.7 nm (Fig. 11b). Only with the combination of carbon dioxide and nitrogen adsorption can complementary and complete pore size and pore volume information be determined. The NLDFT cumulative pore volume data (Fig. 11b) allows one to differentiate between micro- and mesopore volume in a straightforward way.

These examples demonstrate that the application of microscopic methods such as NLDFT and QSDFT allow one to obtain a reliable pore size distribution over the complete micro/mesopore size range. However, it needs to be stressed that this requires that the experimental porous system (i.e. adsorptive/adsorbent system) is compatible with the chosen DFT/MC kernel otherwise erroneous results may be obtained.

5 Summary

Summarizing, the past 20 years have seen major advances in the development of nanoporous materials with ordered

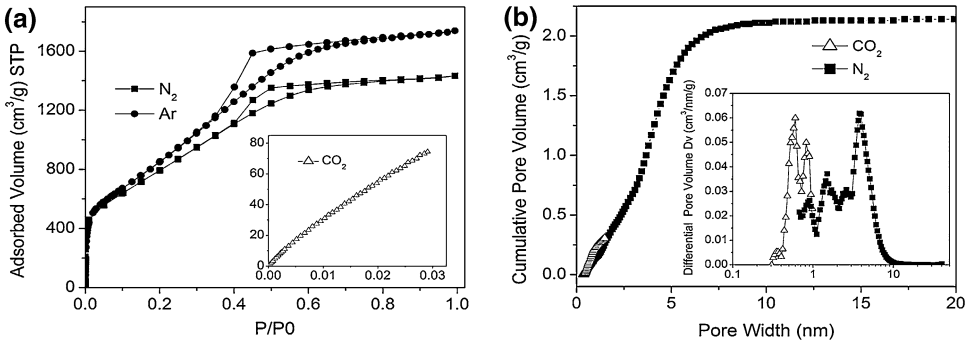

Fig. 11 **a** Nitrogen (77 K), argon (87 K), and carbon dioxide (273 K) adsorption isotherms on a hierarchical graphene oxide material and **b** NLDFT cumulative pore volume and micropore size distribution from the nitrogen and carbon dioxide isotherms. From Zhu et al. (2011)

and well-defined pore structures. Their characterization has required the development of high resolution experimental procedures for the adsorption of various subcritical fluids (e.g. nitrogen at 77 K, argon at 87 K, carbon dioxide at 273 K, krypton at 77 K and 87 K). In the past, nitrogen adsorption at 77 K was the generally accepted method for both micropore and mesopore analysis. However, it is now clear that nitrogen is not an optimal adsorptive for micropore analysis, mainly because of its quadrupole moment, which is largely responsible for the specific interaction with a variety of surface functional groups and exposed ions. Instead, argon (87 K) adsorption is the recommended method for the pore size analysis of microporous materials with polar surface sites. For the characterization of nanoporous carbons with very narrow micropores, it is standard to combine CO_2 (273 K) adsorption with argon or nitrogen adsorption at 87 K and 77 K, respectively.

Microscopic treatments such as DFT and molecular simulation (for a recent review, please see Monson 2012), which can describe the configuration of the adsorbed phase on a molecular level, are now considered to be superior and to provide, compared to the classical, macroscopic methods (e.g. Kelvin equation based approaches, Dubinin–Radushkevitch method) a more reliable approach to pore size analysis over the complete nanopore range. DFT based methods (in particular NLDFT) can be regarded as a standard method for pore size/volume analysis of nanoporous materials (for a review see Landers et al. 2013) Commercial software is now available for many adsorption systems and the DFT method is featured also in international standards (such as ISO 15901-3). With these advanced methods it is now possible to obtain reliable information from both the adsorption and desorption branches of the hysteresis loop which is crucial for pore size characterization of materials consisting of an interconnected micro–mesoporous network. Furthermore, the recently developed QSDFT quantitatively accounts for surface heterogeneity effects, allowing one to obtain a much more reliable pore size assessment of disordered micro- and mesoporous carbons.

However, it needs to be stressed that the application of advanced methods based on DFT and molecular simulation can lead to reasonably accurate evaluation of the pore size distribution only if the given experimental nanoporous system is compatible with the chosen DFT/MC kernel. Hence, classical methods such as the t-methods and alphas-s methods are still very useful in particular if one has to assess the microporosity of disordered experimental systems for which a proper DFT kernel does not exist.

The existing challenges for physical adsorption characterization can be summarized as follows:

- Assessment of surface heterogeneity/surface chemistry of adsorbents. This requires a continuation of the ongoing efforts in developing novel, theoretical and molecular simulation based methods coupled with advanced experimental protocols (which may involve a combination of adsorptives which vary in their sensitivity towards adsorbent surface chemistry/heterogeneity).
- Further progress is needed concerning the investigation of the pore network characteristics of nanoporous materials with hierarchical pore structure (see Sect. 4 and 5). In addition to advances in experimental procedures including the coupling of adsorption with complimentary techniques such as small angle scattering and advanced electronic microscopy approaches (e.g. 3D TEM), the development of even more realistic adsorbent/pore models (beyond the widely used single pore model) is here crucial.
- Characterization of non-rigid, nanoporous materials. This requires an improved understanding of the effects of adsorbent deformation on physical adsorption. A major challenge is the characterization of flexible adsorbents such as MOFs which requires the development of new theoretical approaches based on realistic pore models and also allows one to take into account the non-rigid nature of the adsorbent into account. Some progress has been made during the last few years (see Sect. 1), but this area requires major attention in the near future.

References

Aranovich, G., Donohue, M.: Determining surface areas from linear adsorption isotherms at supercritical conditions. J. Colloid Interface Sci. **194**, 392–397 (1997)

Bakaev, V.A.: Rumpled graphite basal plane as a model heterogeneous carbon surface. J. Chem. Phys. **102**, 1398–1404 (1995)

Bandosz, T.J., Biggs, M.J., Gubbins, K.E., Hattori, Y., Iiyama, T., Kaneko, K., Pikunic, J., Thomson, K.: Molecular models of porous carbons. Chem. Phys. Carbon **28**, 41–228 (2003)

Barton, T.J., Bull, L.M., Klemperer, W.G., Loy, D.A., McEnaney, B., Misono, M., Monson, P.A., Pez, G., Scherer, G.W., Vartuli, J.C., Yaghi, O.M.: Tailored porous materials. Chem. Mater. **11**, 2633–2656 (1999)

Bhatia, S.K.: Density functional theory analysis of the influence of pore wall heterogeneity on adsorption in carbons. Langmuir **18**, 6845–6856 (2002)

Broekhoff, J.C.P., de Boer, J.H.: Studies on pore systems in catalysts: IX. Calculation of pore distributions from the adsorption branch of nitrogen sorption isotherms in the case of open cylindrical pores A. Fundamental equations. J. Catal. **9**, 8–14 (1967a)

Broekhoff, J.C.P., de Boer, J.H.: Studies on pore systems in catalysts: X. Calculations of pore distributions from the adsorption branch of nitrogen sorption isotherms in the case of open cylindrical pores B. Applications. J. Catal. **9**, 15–27 (1967b)

Broekhoff, J.C.P., de Boer, J.H.: Studies on pore systems in catalysts: XIII. Pore distributions from the desorption branch of a nitrogen sorption isotherm in the case of cylindrical pores B. Applications. J. Catal. **10**, 377–390 (1968a)

Broekhoff, J.C.P., de Boer, J.H.: Studies on pore systems in catalysts: XIV. Calculation of the cumulative distribution functions for slit-shaped pores from the desorption branch of a nitrogen sorption isotherm. J. Catal. **10**, 391–400 (1968b)

Cazorla-Amorós, D., Alcañiz-Monge, J., Linares-Solano, A.: Characterization of activated carbon fibers by CO_2 adsorption. Langmuir **12**, 2820–2824 (1996)

Cheng, L.S., Yang, R.T.: Improved Horvath–Kawazoe equations including spherical pore models for calculating micropore size distribution. Chem. Eng. Sci. **49**, 2599–2609 (1994)

Cimino, R., Cychosz, K.A., Thommes, M., Neimark, A.V.: Experimental and theoretical studies of scanning adsorption-desorption isotherms. Colloids Surf. A **437**, 76–89 (2013)

Coasne, B., Galarneau, A., Pellenq, R.J., Di Renzo, F.: Adsorption, intrusion and freezing in porous silica: the view from the nanoscale. Chem. Soc. Rev. **42**, 4141–4171 (2013)

Cole, M.W., Saam, W.F.: Excitation spectrum and thermodynamic properties of liquid films in cylindrical pores. Phys. Rev. Lett. **32**, 985–988 (1974)

Cychosz, K.A., Guo, X., Fan, W., Cimino, R., Gor, G.Y., Tsapatsis, M., Neimark, A.V., Thommes, M.: Characterization of the pore structure of three-dimensionally ordered mesoporous carbons using high resolution gas sorption. Langmuir **28**, 12647–12654 (2012)

DeBoer, J.H.: Structure and properties of porous materials. In: Everett, D.H., Stone, F.S. (eds.) Colston papers. Butterworths, London (1958)

Do, D.D., Do, H.D.: Modeling of adsorption on nongraphitized carbon surface: GCMC simulation studies and comparison with experimental data. J. Phys. Chem. B **110**, 17531–17538 (2006)

Dubinin, M.M., Radushkevitch, L.V.: Dokl. Akak. Nauk. SSSR **55**, 331 (1947)

Dubinin, M.M., Timofeev, D.P.: Zh. Fiz. Khim. **22**, 133 (1948)

Everett, D.H.: Adsorption hysteresis. In: Flood, E.A. (ed.) The Solid–Gas Interface, pp. 1055–1113. Decker, New York (1967)

Everett, D.H., Powl, J.C.: Adsorption in slit-like and cylindrical micropores in the Henry's law region. A model for the microporosity of carbons. J. Chem. Soc., Faraday Trans. **1**(72), 619–636 (1976)

Ferey, G.: Hybrid porous solids. Stud. Surf. Sci. Catal. **168**, 327 (2007)

Findenegg, G.H., Gross, S., Michalski, T.: Pore condensation in controlled-pore glass. An experimental test of the Saam–Cole theory. Stud. Surf. Sci. Catal. **87**, 71–80 (1994)

Findenegg, G.H., Jähnert, S., Müter, D., Prass, J., Paris, O.: Fluid adsorption in ordered mesoporous solids determined by in situ small angle X-ray scattering. Phys. Chem. Chem. Phys. **12**, 7211–7220 (2010)

Furmaniak, S., Terzyk, A.P., Gauden, P.A., Harris, P.J.F., Kowalczyk, P.: The influence of carbon surface oxygen groups on Dubinin–Astakhov equation parameters calculated from CO_2 adsorption isotherm. J. Phys. **22**, 085003 (2010)

García-Martínez, J., Cazorla-Amorós, D., Linares-Solano, A.: Further evidence of the usefulness of CO_2 adsorption to characterize microporous solids. Stud. Surf. Sci. Catal. **128**, 485–494 (2000)

Garrido, J., Linares-Solano, A., Martín-Martínez, J.M., Molina-Sabio, M., Rodríguez-Reinoso, F., Torregrosa, R.: Use of N_2 vs. CO_2 in the characterization of activated carbons. Langmuir **3**, 76–81 (1987)

Gelb, L.D., Gubbins, K.E., Radhakrishnan, R., Sliwinska-Bartkowiak, M.: Phase separation in confined systems. Rep. Prog. Phys. **62**, 1573–1659 (1999)

Gor, G.Y., Thommes, M., Cychosz, K.A., Neimark, A.V.: Quenched solid density functional theory method for characterization of mesoporous carbons by nitrogen adsorption. Carbon **50**, 1583–1590 (2012)

Gor, G.Y., Neimark, A.V.: Adsorption-induced deformation of mesoporous solids: macroscopic approach and density functional theory. Langmuir **27**, 6926–6931 (2011)

Gor, G.Y., Paris, O., Prass, J., Russo, P.A., Carott Ribeiro, M.L., Neimark, A.V.: Adsorption of *n*-pentane on mesoporous silica and adsorbent deformation. Langmuir **29**, 8601–8608 (2013)

Gregg, S.J., Sing, K.S.W.: Adsorption. Surface Area and Porosity. Academic Press, London (1982)

Grosman, A., Ortega, C.: Capillary condensation in porous materials. Hysteresis and interaction without pore blocking/percolation process. Langmuir **24**, 3977–3986 (2008)

Gubbins, K.E.: Theory and simulation of adsorption in micropores. In: Fraissard, J., Conner, C.W. (eds.) Physical Adsorption: Experiment, Theory and Applications, pp. 65–103. Kluwer Academic Publishers, The Netherlands (1997)

Hartmann, M., Jung, D.: Biocatalysis with enzymes immobilized on mesoporous hosts: the status quo and future trends. J. Mater. Chem. **20**, 844–857 (2010)

Hirscher, M., Panella, B., Schmitz, B.: Metal–organic frameworks for hydrogen storage. Microporous Mesoporous Mater. **129**, 335–339 (2010)

Horvath, G., Kawazoe, K.: Method for the calculation of effective pore size distribution in molecular sieve carbon. J. Chem. Eng. Japan **16**, 470–475 (1983)

Horikawa, T., Sekida, T., Hayashi, J., Katoh, M., Do, D.D.: A new adsorption–desorption model for water adsorption in porous carbons. Carbon **49**, 416–424 (2011)

Hoffmann, F., Cornelius, M., Morell, M., Fröba, M.: Periodic mesoporous organosilicas: past, presence and future. J. Nanosci. Nanotechn. **6**, 265–288 (2006)

Hung, F.R., Bhattacharya, S., Coasne, B., Thommes, M., Gubbins, K.E.: Argon and krypton adsorption on templated mesoporous silicas: molecular simulation and experiment. Adsorption **13**, 425–437 (2007)

Inayat, A., Knoke, I., Spieker, E., Schwieger, W.: Assemblies of mesoporous FAU-type zeolite nanosheets. Agew. Chem. Int. Ed. **51**, 1965–1992 (2012)

Jagiello, J., Thommes, M.: Comparison of DFT characterization methods based on N_2, Ar, CO_2, and H_2 adsorption applied to carbons with various pore size distributions. Carbon **42**, 1227–1232 (2004)

Jagiello, J., Olivier, J.P.: A simple two-dimensional NLDFT model of gas adsorption in finite carbon pores. Application to pore structure analysis. J. Phys. Chem. C **113**, 19382–19385 (2009)

Jagiello, J., Olivier, J.P.: 2D-NLDFT adsorption models for carbon slit-shaped pores with surface energetical heterogeneity and geometrical corrugation. Carbon **55**, 70–80 (2013)

Jähnert, S., Müter, D., Prass, J., Zickler, G.A., Paris, O., Findenegg, G.H.: Pore structure and fluid sorption in ordered mesoporous silica. I. Experimental study by in situ small-angle X-ray scattering. J. Phys. Chem. C **113**, 15201–15210 (2009)

Jaroniec, M., Solovyov, L.A.: Improvement of the Kruk–Jaroniec–Sayari method for pore size analysis of ordered silica with cylindrical mesopores. Langmuir **22**, 6757–6760 (2006)

Kaneko, K., Roh, T., Fujimori, T.: Collective interactions of molecules with an interfacial solid. Chem. Lett. **41**, 466–475 (2012)

Kaneko, K., Hanzawa, Y., Iiyama, T., Kanda, T., Suzuki, T.: Cluster-mediated water adsorption on carbon nanopores. Adsorption **5**, 7–13 (1999)

Kim, T.W., Ryoo, R., Kruk, M., Gierszal, K.P., Jaroniec, M., Kamiya, S., Terasaki, O.: Tailoring the pore structure of SBA-16 silica molecular sieve through the use of copolymer blends and control of synthesis temperature and time. J. Phys. Chem. B **108**, 11480–11489 (2004)

Kleitz, F.: Ordered mesoporous materials. In: Ertl, G., Koezinger, H., Schueth, F., Weitkamp, J. (eds.) Handbook of Heterogenous Catalysis, pp. 178–219. Wiley, Weinheim (2008)

Kleitz, F., Bérubé, F., Guillet-Nicolas, R., Yang, C.-M., Thommes, M.: Probing adsorption, pore condensation, and hysteresis behavior of pure fluids in three-dimensional cubic mesoporous KIT-6 silica. J. Phys. Chem. C **114**, 9344–9355 (2010)

Kleitz, F., Choi, S.H., Ryoo, R.: Cubic Ia3d large mesoporous silica: synthesis and replication to platinum nanowires, carbon nanorods and carbon nanotubes. Chem. Commun. **17**, 2136–2137 (2003)

Krause, K.M., Thommes, M., Brett, M.J.: Pore analysis of obliquely deposited nanostructures by krypton gas adsorption at 87 K. Microporous Mesoporous Mater. **143**, 166–173 (2011)

Kresge, C.T., Roth, W.J.: The discovery of mesoporous molecular sieves from the twenty year perspective. Chem. Soc. Rev. **42**, 3663–3670 (2013)

Kruk, M., Celer, E.B., Matos, J.R., Pikus, S., Jaroniec, M.: Synthesis of FDU-1 silica with narrow pore size distribution and tailorable pore entrance size in the presence of sodium chloride. J. Phys. Chem. B **109**, 3838–3843 (2005)

Kruk, M., Jaroniec, M., Sayari, A.: Application of large pore MCM-41 molecular sieves to improve pore size analysis using nitrogen adsorption measurements. Langmuir **13**, 6267–6273 (1997)

Landers, J., Gor, G.Y., Neimark, A.V.: Density functional theory methods for characterization of porous materials. Colloids Surf. A **437**, 3–32 (2013)

Lässig, D., Lincke, J., Moellmer, J., Reichenbach, C., Moeller, A., Gläser, R., Kalies, G., Cychosz, K.A., Thommes, M., Staudt, R., Krautscheid, H.: A microporous copper metal-organic framework with high H_2 and CO_2 adsorption capacity at ambient pressure. Angew. Chem. Int. Ed. **50**, 10344–10348 (2011)

Lastoskie, C., Gubbins, K.E., Quirke, N.: Pore size distribution analysis of microporous carbons: a density functional theory approach. J. Phys. Chem. **97**, 4786–4796 (1993)

Li, H., Eddaoudi, M., O'Keeffe, M., Yaghi, O.M.: Design and synthesis of an exceptionally stable and highly porous metal–organic framework. Nature **402**, 276–279 (1999)

Li, K., Valla, J., Garcia-Martinez, J.: Realizing the commercial potential of hierarchical zeolites: new opportunities in catalytic cracking. ChemCatChem (2013). doi:10.1002cctc.2013.201300345

Libby, B., Monson, P.A.: Adsorption/desorption hysteresis in inkbottle pores: a density functional theory and Monte Carlo simulation study. Langmuir **20**, 4289–4294 (2004)

Liu, J.-C., Monson, P.A.: Does water condense in carbon pores? Langmuir **21**, 10219–10225 (2005)

Liu, H., Seaton, N.A.: Determination of the connectivity of porous solids from nitrogen sorption measurements—III. Solids containing large mesopores. Chem. Eng. Sci. **49**, 1869–1878 (1994)

Liu, H., Zhang, L., Seaton, N.A.: Sorption hysteresis as a probe of pore structure. Langmuir **9**, 2576–2582 (1993)

Lowell, S., Shields, J., Thomas, M.A., Thommes, M.: Characterization of Porous Solids and Powders: Surface Area. Pore Size and Density. Springer, Amsterdam (2004)

Lodewyckx, P., Vansant, E.F.: Water isotherms of activated carbons with small amounts of surface oxygen. Carbon **37**, 1647–1649 (1999)

Lodewyckx, P., Raymundo-Pinera, E., Vaclavikova, M., Berezovska, I., Thommes, M., Beguin, F., Dobos, G.: Suggested improvements in the parameters used for describing the low relative pressure region of the water vapour isotherms of activated carbons. Carbon **60**, 556–558 (2013)

Lucena, S.M.P., Paiva, C.A.S., Silvino, P.F.G., Azevedo, D.C.S., Cavalcante, C.L.: The effect of heterogeneity in the randomly etched graphite model for carbon pore size characterization. Carbon **48**, 2554–2565 (2010)

Mascotto, S., Wallacher, D., Brandt, A., Hauss, T., Thommes, M., Zickler, G.A., Funari, S., Timmann, A., Smarsly, B.: Analysis of microporosity in ordered mesoporous hierarchically structured silica by combining physisorption with in situ small-angle scattering (SAXS and SANS). Langmuir **25**, 12670–12681 (2009)

Mason, G.: The effect of pore space connectivity on the hysteresis of capillary condensation in adsorption–desorption isotherms. J. Colloids Interface Sci. **88**, 36–46 (1982)

Mintova, S., Cejka, J.: Micro/mesoporous composites. Stud. Surf. Sci. Catal. **168**, 301–326 (2007)

Moellmer, J., Celer, E.B., Luebke, R., Cairns, A.J., Staudt, R., Eddaoudi, M., Thommes, M.: Insights on adsorption characterization of metal-organic frameworks: a benchmark study on the novel soc-MOF. Microporous Mesoporous Mater. **129**, 345–353 (2010)

Möller, K., Bein, T.: Pore within pores—how to craft ordered hierarchical zeolites. Science **333**, 297–298 (2011)

Monson, P.A.: Understanding adsorption/desorption hysteresis for fluids in mesoporous materials using simple molecular models and classical density functional theory. Microporous Mesoporous Mater. **160**, 47–66 (2012)

Monson, P.A.: Contact angles, pore condensation and hysteresis: insights from a simple molecular model. Langmuir **24**, 12295–12302 (2008)

Naumov, S., Khokhlov, A., Valiullin, R., Karger, J., Monson, P.A.: Understanding capillary condensation and hysteresis in porous silicon: network effects within independent pores. Phys. Rev. E **78**, 060601 (2008)

Morishige, K., Tateishi, M., Hirose, F.: Change in desorption mechanism from pore blocking to cavitation with temperature for nitrogen in ordered silica with cagelike pores. Langmuir **22**, 9220–9224 (2006)

Myasaka, K., Hano, H., Kubota, Y., Lin, Y., Ryoo, R., Takata, M., Kitagawa, S., Neimark, A.V., Terasaki, O.: A stand-alone

mesoporous crystal structure model from in situ X-ray diffraction: nitrogen adsorption on 3D cagelike mesoporous silica SBA-16. Chem. Eur. J. **18**, 10300 (2012)

Na, K., Jo, C., Kim, J., Cho, K., Jung, J., Seo, Y., Messinger, R.J., Chmelka, B.F., Ryoo, R.: Directing zeolite structures into hierarchically nanoporous architectures. Science **333**, 328–332 (2011)

Neimark, A.V.: The method of indeterminate Lagrange multipliers in nonlocal density functional theory. Langmuir **11**, 4183–4184 (1995)

Neimark, A.V.: Percolation theory of capillary hysteresis phenomena and its application for characterization of porous solids. Stud. Surf. Sci. Catal. **62**, 67–74 (1991)

Neimark, A.V., Ravikovitch, P.I.: Capillary condensation in MMS and pore structure characterization. Micropor. Mesopor. Mat. **44**, 697–707 (2001)

Neimark, A.V., Ravikovitch, P.I., Vishnyakov, A.: Bridging scales from molecular simulations to classical thermodynamics: density functional theory of capillary condensation in nanopores. J. Phys. **15**, 347–365 (2003)

Neimark, A.V., Lin, Y., Ravikovitch, P.I., Thommes, M.: Quenched solid density functional theory and pore size analysis of micro-mesoporous carbons. Carbon **47**, 1617–1628 (2009)

Neimark, A.V., Sing, K.S.W., Thommes, M.: Surface area and porosity. In: Ertl, G., Koezinger, H., Schueth, F., Weitkamp, J. (eds.) Handbook of Heterogeneous Catalysis, pp. 721–737. Wiley, New York (2008)

Neimark, A.V., Coudert, F.X., Boutin, A., Fuchs, A.H.: Stress-based model for the breathing of metal–organic framework. Phys. Chem. Lett. **1**, 445–449 (2010)

Nguyen, T.X., Cohaut, N., Bae, J.-S., Bhatia, S.K.: New method for atomistic modeling of the microstructure of activated carbons using hybrid reverse Monte Carlo simulation. Langmuir **24**, 7912–7922 (2008)

Nguyen, P.T.M., Fan, C., Do, D.D., Nicholson, D.: On the cavitation-like pore blocking in ink-bottle pore: evolution of hysteresis loop with neck size. J. Phys. Chem. C **117**, 5475–5484 (2013a)

Nguyen, P.T., Do, D.D., Nicholson, D.: Simulation study of hysteresis of argon adsorption in a conical pore and a constricted cylindrical pore. J. Colloid Interface Sci. **396**, 242–250 (2013b)

Ohba, T., Kanoh, H., Kaneko, K.: Cluster-growth-induced water adsorption in hydrophobic carbon nanopores. J. Phys. Chem. B **108**, 14964–14969 (2004)

Olivier, J.P.: Improving the models used for calculating the size distribution of micropore volume of activated carbons from adsorption data. Carbon **36**, 1469–1472 (1998)

Olivier, J.P., Conklin, W.B., Szombathely, M.V.: Determination of pore size distribution from density functional theory: a comparison of nitrogen and argon results. Stud. Surf. Sci. Catal. **87**, 81–89 (1994)

Parlar, M., Yortsos, Y.C.: Percolation theory of vapor adsorption–desorption processes in porous materials. J. Colloid Interface Sci. **124**, 162–176 (1988)

Pauporté, T., Rathousky, J.: Electrodeposited mesoporous ZnO thin films as efficient photocatalysts for the degradation of dye pollutants. J. Phys. Chem. C **111**, 7639–7644 (2007)

Pérez-Ramírez, J., Mitchell, S., Verboekend, D., Milina, M., Michels, N.-L., Krumeich, F., Marti, N., Erdmann, M.: Expanding the horizons of hierarchical zeolites: beyond laboratory curiosity towards industrial revolution. ChemCatChem **3**, 1731–1734 (2011)

Rasmussen, C.J., Vishnyakov, A., Thommes, M., Smarsly, B.M., Kleitz, F., Neimark, A.V.: Cavitation in metastable liquid nitrogen confined to nanoscale pores. Langmuir **26**, 10147–10157 (2010)

Ravikovitch, P.I., Neimark, A.V.: Density functional theory of adsorption in spherical cavities and pore size characterization of templated nanoporous silicas with cubic and three-dimensional hexagonal structures. Langmuir **18**, 1550–1560 (2002a)

Ravikovitch, P.I., Neimark, A.V.: Experimental confirmation of different mechanisms of evaporation from ink-bottle type pores: equilibrium, pore blocking, and cavitation. Langmuir **18**, 9830–9837 (2002b)

Ravikovitch, P.I., Vishnyakov, A., Russo, R., Neimark, A.V.: Unified approach to pore size characterization of microporous carbonaceous materials from N_2, Ar, and CO_2 adsorption isotherms. Langmuir **16**, 2311–2320 (2000)

Reichenauer, G., Scherer, G.W.: Nitrogen adsorption in compliant materials. J. Non-Cryst. Solids **277**, 162–172 (2000)

Reichenauer, G.: Micropore adsorption dynamics in synthetic hard carbons. Adsorption **11**, 467–471 (2005)

Rios, R.V.R.A., Silvestre-Albero, J., Sepúlveda-Escribano, A., Molina-Sabio, M., Rodríguez-Reinoso, F.: Kinetic restrictions in the characterization of narrow microporosity in carbon materials. J. Phys. Chem. C **111**, 3803–3805 (2007)

Rojas, F., Kornhauser, I., Felipe, C., Esparza, J.M., Cordero, S., Domínguez, A., Riccardo, J.L.: Capillary condensation in heterogeneous mesoporous networks consisting of variable connectivity and pore-size correlation. Phys. Chem. Chem. Phys. **4**, 2346–2355 (2002)

Roth, W.J., Vartuli, J.C.: Synthesis of mesoporous molecular sieves. Stud. Surf. Sci. Catal. **157**, 91–110 (2005)

Rouquerol, J., Avnir, D., Fairbridge, C.W., Everett, D.H., Haynes, J.H., Pernicone, N., Ramsay, J.D.F., Sing, K.S.W., Unger, K.K.: Recommendations for the characterization of porous solids. Pure Appl. Chem. **66**, 1739–1748 (1994)

Rouquerol, J., Baron, G., Denoyel, R., Giesche, H., Groen, J., Klobes, P., Levitz, P., Neimark, A.V., Rigby, S., Skudas, R., Sing, K., Thommes, M., Unger, K.: Liquid intrusion and alternative methods for the characterization of macroporous materials. Pure Appl. Chem. **84**, 107–136 (2012)

Rouquerol, F., Rouquerol, J., Sing, K.S.W., Llewellyn, P., Maurin, G.: Adsorption by Powders and Porous Solids. Academic Press, London (2013)

Rouquerol, J., Llewellyn, P., Rouquerol, F.: Is the BET equation applicable to micropore adsorbents? Stud. Surf. Sci. Catal. **160**, 49–56 (2007)

Saito, A., Foley, H.C.: Curvature and parametric sensitivity in models for adsorption in micropores. AIChE J. **37**, 429–436 (1991)

Sarkisov, L., Monson, P.A.: Modeling of adsorption and desorption in pores of simple geometry using molecular dynamics. Langmuir **17**, 7600–7604 (2001)

Sel, O., Brandt, A., Wallacher, D., Thommes, M., Smarsly, B.: Pore hierarchy in mesoporous silicas evidenced by in situ SANS during nitrogen physisorption. Langmuir **23**, 4724–4727 (2007)

Seaton, N.A., Walton, J.P.R.B., Quirke, N.: A new analysis method for the determination of the pore size distribution of porous carbons from nitrogen adsorption measurements. Carbon **27**, 853–861 (1989)

Serrano, D.P., Aguado, J., Morales, G., Rodríguez, J.M., Peral, A., Thommes, M., Epping, J.D., Chmelka, B.F.: Molecular and meso- and macroscopic properties of hierarchical nanocrystalline ZSM-5 zeolite prepared by seed silanization. Chem. Mater. **21**, 641–654 (2009)

Shpeizer, B.G., Bakhmutov, V.I., Clearfield, A.: Supermicroporous alumina–silica zinc oxides. Microporous Mesoporous Mater. **90**, 81–86 (2006)

Shpeizer, B.G., Bakhmoutov, V.I., Zhang, P., Prosvirin, A.V., Dunbar, K.R., Thommes, M., Clearfield, A.: Transition metal–alumina/silica supermicroporous composites with tunable porosity. Colloids Surfaces A **357**, 105–115 (2010)

Shen, J., Monson, P.A.: A molecular model of adsorption in a dilute semiflexible porous network. Mol. Phys. **100**, 2031–2039 (2002)

Silvestre-Albero, J., Silvestre-Albero, A., Rodríguez-Reinoso, F., Thommes, M.: Physical characterization of activated carbons with narrow microporosity by nitrogen (77.4 K), carbon dioxide (273 K) and argon (87.3 K) adsorption in combination with immersion calorimetry. Carbon **50**, 3128–3133 (2012)

Sing, K.S.W., Everett, D.H., Haul, R.A.W., Moscou, L., Pierotti, R.A., Rouquerol, J., Siemieniewska, T.: Reporting physisorption data for gas/solid systems with special reference to the determination of surface area and porosity. Pure Appl. Chem. **57**, 603–619 (1985)

Soares Maia, D.A., de Oliveira, J.C.A., Toso, J.P., Sapag, K., López, R.H., Azevedo, D.C.S., Cavalcante, C.L., Zgrablich, G.: Characterization of the PSD of activated carbons from peach stones for separation of combustion gas mixtures. Adsorption **17**, 853–861 (2011)

Tanaka, H., Hiratsuka, T., Nishiyama, N., Mori, K., Miyahara, M.T.: Capillary condensation in mesoporous silica with surface roughness. Adsorption **19**, 631–641 (2013)

Stoeckli, F., Lavanchy, A.: The adsorption of water by active carbons, in relation to their chemical and structural properties. Carbon **38**, 475–477 (2000)

Tarazona, P.: Free-energy density functional for hard spheres. Phys. Rev. A **31**, 2672–2679 (1985)

Tarazona, P., Evans, R.: A simple density functional theory for inhomogeneous liquids. Mol. Phys. **52**, 847–857 (1984)

Thommes, M.: Physical adsorption characterization of nanoporous materials. Chem. Ing. Tech. **82**, 1059–1073 (2010)

Thommes, M., Findenegg, G.H.: Pore condensation and critical-point shift of a fluid in controlled-pore glass. Langmuir **10**, 4270–4277 (1994)

Thommes, M.: Physical adsorption characterization of ordered and amorphous mesoporous materials. In: Lu, G.Q., Zhao, X.S. (eds.) Nanoporous Materials Science and Engineering, pp. 317–364. World Scientific, London (2004)

Thommes, M.: Textural characterization of zeolites and ordered mesoporous materials by physical adsorption. Stud. Surf. Sci. Catal. **168**, 495–523 (2007)

Thommes, M., Cychosz, K.A., Neimark, A.V.: Advanced physical adsorption characterization of nanoporous carbons. In: Tascon, J.M.D. (ed.) Novel Carbon Adsorbents, pp. 107–145. Elsevier, Oxford (2012a)

Thommes, M., Mitchell, S., Pérez-Ramírez, J.: Surface and pore structure assessment of hierarchical MFI zeolites by advanced water and argon sorption studies. J. Phys. Chem. C **116**, 18816–18823 (2012b)

Thommes, M., Nishyama, N., Tanaka, S.: Aspects of a novel method for the pore size analysis of thin silica films based on krypton adsorption at liquid argon temperature (87.3 K). Stud. Surf. Sci. Catal. **165**, 551–554 (2007)

Thommes, M., Smarsly, B., Groenewolt, M., Ravikovitch, P.I., Neimark, A.V.: Adsorption hysteresis of nitrogen and argon in pore networks and characterization of novel micro- and mesoporous silicas. Langmuir **22**, 756–764 (2006)

Thommes, M., Morlay, C., Ahmad, R., Joly, J.P.: Assessing surface chemistry and pore structure of active carbons by a combination of physisorption (H_2O, Ar, N_2, CO_2). XPS and TPD-MS. Adsorption **17**, 653–661 (2011)

Thommes, M., Morell, J., Cychosz, K.A., Fröba, M.: Combining nitrogen, argon, and water adsorption for advanced characterization of ordered mesoporous carbons (CMKs) and periodic mesoporous organosilicas (PMOs). Langmuir (2013). doi:10.1021/la402832b

Thommes, M., Köhn, R., Fröba, M.: Sorption and pore condensation behavior of pure fluids in mesoporous MCM-48 silica, MCM-41 silica, SBA-15 silica and controlled pore glass at temperatures above and below the bulk triple point. Appl. Surf. Sci. **196**, 239–249 (2002)

Thomson, K.T., Gubbins, K.E.: Modeling structural morphology of microporous carbons by reverse Monte Carlo. Langmuir **16**, 5761–5773 (2000)

Turner, A.R., Quirke, N.A.: Grand canonical Monte Carlo study of adsorption on graphitic surfaces with defects. Carbon **36**, 1439–1446 (1998)

Valiullin, R., Naumov, S., Galvosas, P., Karger, J., Woo, H.J., Porcheron, F., Monson, P.A.: Exploration of molecular dynamics during transient sorption of fluids in mesoporous materials. Nature **443**, 965–968 (2006)

Valiullin, R., Kaerger, J.: The impact of mesopores on mass transfer in nanoporous materials: evidence of diffusion measurement by NMR. Chem. Ing. Tech. **83**, 166 (2011)

Van Bemmelen, J.M.: Die absorption das wasser in den kolloiden, besonders in dem gel der kieselsäure. Z. Anorg. Allg. Chem. **13**, 233–356 (1897)

Vishnyakov, A., Neimark, A.V.: Monte Carlo simulation test of pore blocking effects. Langmuir **19**, 3240–3247 (2003)

Vishnyakov, A., Ravikovitch, P.I., Neimark, A.V.: Molecular level models for CO_2 sorption in nanopores. Langmuir **15**, 8736–8742 (1999)

Wall, G.C., Brown, R.J.C.: The determination of pore-size distributions from sorption isotherms and mercury penetration in interconnected pores: the application of percolation theory. J. Colloid Interface Sci. **82**, 141–149 (1981)

Woo, H.-J., Sarkisov, L., Monson, P.A.: Mean-field theory of fluid adsorption in a porous glass. Langmuir **17**, 7472–7475 (2001)

Zhang, X., Liu, D., Xu, D., Asahina, S., Cychosz, K.A., Agrawal, K.V., AlWahedi, Y., Bhan, A., AlHashimi, S., Terasaki, O., Thommes, M., Tsapatsis, M.: Synthesis of self-pillared nanosheets by repetitive branching. Science **336**, 1684–1687 (2012)

Zhao, D., Wang, Y.: The synthesis of mesoporous molecular sieves. Stud. Surf. Sci. Catal. **168**, 241–300 (2007)

Zhu, Y., Murali, S., Stoller, M.D., Ganesh, K.J., Cai, W., Ferreira, P.J., Pirkle, A., Wallace, R.M., Cychosz, K.A., Thommes, M., Su, D., Stach, E.A., Ruoff, R.S.: Carbon-based supercapacitors produced by activation of graphene. Science **332**, 1537–1541 (2011)